Arctic Observation and Reanalysis Integrated System

A New Data Product for Validation and Climate Study

BY MATTHEW W. CHRISTENSEN, ALI BEHRANGI, TRISTAN S. L'ECUYER, NORMAN B. WOOD, MATTHEW D. LEBSOCK, AND GRAEME L. STEPHENS

In recent decades, sea ice and snow cover extent has declined across the Arctic. The melting has been confirmed using numerous observational tools. While climate models also tend to predict melting trends, a wide range of projections manifest due to uncertainties in Arctic processes. Causes for the rapid loss of sea ice are complex and linked to the surface radiation budget, possibly through cloud and sea ice feedbacks. Furthermore, the rapid degradation (through warming and melting of permafrost) of delicate ecosystems that lock vast quantities of carbon dioxide under the crust of the Arctic demands urgent attention. It is therefore essential to monitor and improve current assessments of the surface energy budget in order to gain a better understanding of how climate change may manifest in the future.

To improve assessments of the Arctic energy budget for validation and scientific study, we have developed the Arctic Observation and Reanalysis Integrated System (ArORIS), which merges numerous state-of-the-art satellite, reanalysis, and in situ datasets from peer-reviewed products using a conventional grid and name-labeling framework. It is primarily geared for scientific inquiry, product validation, and assessment of the radiation and moisture budgets in the Arctic.

To study the complex interactive processes among radiation, clouds, precipitation, sea ice, and snow (to name a few), numerous disparate datasets are required. Being confronted by the large number of satellite instruments and modeling-derived products makes conducting science more difficult through the laborious task of collecting and collocating multiple data streams onto a common grid. Here, we develop ArORIS to bypass the data acquisition and collocation processes for several key products through applying a common naming and grid convention so that analysis can be conducted seamlessly for the Arctic region.

The purpose of this paper is to provide an overview of the ArORIS dataset and to show a few applications that demonstrate the value of ArORIS for validation, science, and assessment studies of the surface energy budget in a rapidly changing Arctic climate.

AFFILIATIONS: CHRISTENSEN—Colorado State University, Fort Collins, Colorado, and Jet Propulsion Laboratory, California Institute of Technology, Pasadena, California; BEHRANGI, LEBSOCK, AND STEPHENS—Jet Propulsion Laboratory, California Institute of Technology, Pasadena, California; L'ECUYER—Department of Atmospheric and Oceanic Sciences, University of Wisconsin—Madison, Madison, Wisconsin; WOOD—Cooperative Institute for Meteorological Satellite Studies, University of Wisconsin—Madison, Madison, Wisconsin

CORRESPONDING AUTHOR: M. W. Christensen, Science and Technology Facilities Council, Rutherford Appleton Laboratory, Didcot OX11 0QX, United Kingdom

E-mail: matt.christensen@jpl.nasa.gov

DOI:10.1175/BAMS-D-14-00273.1

ARORIS DATASET OVERVIEW. ArORIS integrates products from several satellite, reanalysis, and ground-based data sources. Where possible, the following quantities are included: satellite-retrieved cloud properties (e.g., vertical cloud fraction, droplet effective radius, optical depth, and liquid water path), radiation fluxes (top and bottom of atmosphere), surface precipitation, and sea and snow ice extents. Corresponding quantities are also provided from several reanalysis products. Furthermore, aerosol optical depths and thermodynamic and wind profiles are provided in selected satellite and reanalysis products.

The list of matched products in ArORIS is displayed in Table 1. Detailed information about primary

Table 1. Geophysical quantities included in the JPL-ArORIS.

Dataset	Primary Variables[1]	Product	Period	Instrument Resolution	Note	Distribution Ctr. and Acquisition Website
Satellite Products						
AIRS (Atmospheric Infrared Sounder)	cloud, meteorol.	AIRX3STM	2002–13	14 km	high spectral resolution spectrometer	NASA GODDARD disc.sci.gsfc.nasa.gov
CERES (Clouds and the Earth's Radiant Energy System)	radiation	EBAF V2.7	2002–13	20 km	broadband scanning radiometer	NASA LANGELY ceres.larc.nasa.gov
CloudSat	cloud, radiation, precip.	GEOPROF GEOPROF-lidar FLXHR-lidar RAIN-PROFILE SNOW-PROFILE	2006–11	1.4 km	radar and lidar (CALIPSO)	CIRA www.cloudsat.cira.colostate.edu
CloudSat-ERB (Earth Radiation Budget)	radiation	FLXHR-lidar	2006–11	1.4 km	radar and lidar (CALIPSO)	contact Tristan L'Ecuyer
MODIS (MODerate resolution Imaging Spectro-radiometer)	cloud	MYD08_M3	2002–13	1 km	scanning spectro-radiometer	NASA GODDARD https://ladsweb.nascom.nasa.gov
(A)ATSR (Advanced Along Track Scanning Radiometer)	cloud	ORAC – 2 Cloud_CCI version 2	1995–2012	1 km	Satellites: ATSR-2 and AATSR	CEDA www.ceda.ac.uk
GEWEX-SRB (Global Energy and Water Exchanges Project—Surface Radiation Budget)	radiation	REL3.1 LW REL3.0 SW	1983–2008	1°	ISCCP cloud and GMAO input to radiation algorithm	NASA LANGLEY https://eosweb.larc.nasa.gov
GRACE (Gravity Recovery And Climate Experiment)	water storage	CSR, JPL, GFZ	2003–13	1°	Ranging polar orbiting twin-satellites	NASA JPL grace.jpl.nasa.gov

[1] The following words were shortened for space: radiation (shortwave and longwave atmospheric radiation fluxes for the top and bottom of atmosphere), precip (surface precipitation rate), meteorol (vertically resolved meteorological quantities, such as temperature, humidity, and pressure), cloud (properties such as cloud optical depth, effective radius, height, etc.), and climate indices (such as El Niño–Southern Oscillation, Pacific decadal oscillation, North Atlantic Oscillation, etc.).

NSIDC (National Snow and Ice Data Center)	snow and ice	EASE-Grid	2002–13	25 km	Passive microwave satellites	NSIDC nsidc.org
CMAP (CPC Merged Analysis of Precipitation)	precip.	standard	1979–2011	2.5°	Passive microwave + IR satellites	NOAA esrl.noaa.gov
GPCP (Global Precipitation Climatology Project)	precip	V2.2	1979–2010	2.5°	Gauge + IR + microwave satellites	NASA www.gewex.org
Reanalysis Products						
ASR (Arctic System Reanalysis)	radiation, precip.	Interim	2000–10	30 km	WRF-VAR and PWRF	NCAR https://climatedataguide.ucar.edu
ECMWF (European Centre for Medium-range Weather Forecasting)	radiation, cloud, precip.	Interim	2002–13	0.75°	2 times daily data	ECMWF apps.ecmwf.int
MERRA (Modern Era Retrospective Analysis For Research and Applications)	radiation, cloud, precip.	IAU 2D	1980–2013	1.25°	Monthly data	NASA GODDARD disc.sci.gsfc.nasa.gov
NCEP (National Centers for Environmental Prediction)	radiation, cloud, precip., meteorol.	DOE-Reanalysis 2	2000–13	1.25°	Daily averaged data	NOAA esrl.noaa.gov
Assimilated (Satellite + Reanalysis) Products						
GLDAS (Global Land Data Assimilation System)	water budget	NOAH025_M.020	2002–13	0.25°	Monthly data	NASA GODDARD disc.sci.gsfc.nasa.gov
MACC (Monitoring Atmospheric Composition and Climate)	aerosol	ECMWF	2006–13	1.25°	6 times daily	ECMWF http://apps.ecmwf.int/datasets/
Ground Observations						
ARM (Atmospheric Radiation Measurement)	radiation, cloud	ARMBE ARSCL	1998–2011	N/A	North Slope Alaska at Barrow	ARM climate research facility www.archive.arm.gov

GCNET (Greenland Climate Network)	radiation		1996–2013	N/A	23 Gauges over Greenland	CIRES cires.colorado.edu
GPCC (Global Precipitation Climatology Centre)	precip.	Full V6	1901–2010	0.5°	Rain gauge network	NOAA www.esrl.noaa.gov
AMVER (Automated Mutual-Assistance Vessel Rescue System)	ship traffic	N/A	2006–10	0.25°	Daily data	AMVER www.amver.com
Climate Variability Indices						
NOAA (National Oceanic and Atmospheric Administration)	climate indices	N/A	1885–2013	N/A	Monthly data	NOAA www.esrl.noaa.gov

variables, the spatial and temporal sampling, and data acquisition is provided in the table. Most of these products have been published in peer-reviewed articles and rebinned via linear spatial interpolation to match the common grid used here.

All of the products in ArORIS have been matched to the same spatial grid where the temporal sampling period has been preserved in all datasets. Most reanalysis products span from 1979 to the present day, while the period for the satellite instruments on the *Aqua* satellite is from 2002 to the present day, and June 2006 to 2011 for *CloudSat* and *CALIPSO* products. Observations from the International Satellite Cloud Climatology Project (ISCCP) are used to produce the longer-term (1983–2008) GEWEX-SRB satellite product.

The spatial and temporal resolution is based on the sampling frequency of the active sensors (e.g., the *CloudSat* radar and *CALIPSO* lidar) in the A-Train constellation of satellites. The A-Train orbits the Earth in a sun-synchronous trajectory, lapping the equator 14.5 times a day at approximately 1:30 a.m./p.m. and spending most of its observation period at higher latitudes. Active sensors are pointed at/near nadir and can provide detailed measurements of the vertical structure of cloud and aerosol, albeit only over a narrow slice of the atmosphere. As a consequence, the horizontal spatial coverage is sampled at a significantly smaller frequency compared to passive imagers. Therefore, to accommodate both data products, the selected grid size needs to span a large enough area to contain a sufficient number of samples. Furthermore, because the peak of the A-train orbit occurs at 82.5°N/S, the measurements provided by the active sensors do not extend beyond these latitudes. Because the passive imagers (e.g., CERES, MODIS, AIRS, GEWEX-SRB, AATSR) provide complete coverage over the poles, these data are provided in the ArORIS product. However, to make comparisons among all of the products, we restrict the latitude range to 70°–82.5°N for the results reported here; the complete ArORIS product spans the latitude range 60°–90°N.

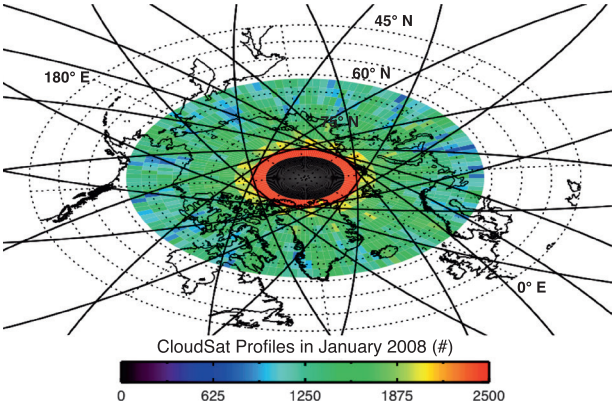

Fig. 1. Number of *CloudSat* profiles binned into 2.5° × 2.5° regions using Jan 2008 observations over 60°N–90°N. Black lines are individual orbits made by *CloudSat* for one day of observations.

To provide sufficient sampling over the Arctic, data are averaged into 2.5° × 2.5° latitude/longitude bins at monthly intervals. The spatial resolution was chosen in order to collect a large enough number of *CloudSat/CALIPSO* samples to produce reasonable statistics of the selected variables. The constant latitude scaling is complemented by the heavily weighted sampling of A-Train sensors at high latitudes where the size of the grids are smaller due to the curvature of the Earth. Figure 1 demonstrates this effect whereby the total number of *CloudSat* profiles, shown for January 2008, increase toward the poles despite the smaller size of the grid area. Each grid cell contains between 1,000 and 2,500 *CloudSat* profiles for a given month. Caution should be used when applying this relatively coarse grid to regions with strong gradients for some of the selected variables—for example, precipitation along coastal areas. Therefore, we provide composite products for land and ocean separately, as well as day and night conditions when they are available. Care should also be used when making comparisons between quantities that have been retrieved using different techniques and or spatial/temporal resolutions. We therefore recommend users of ArORIS to become familiar with the standard product documentation of each dataset.

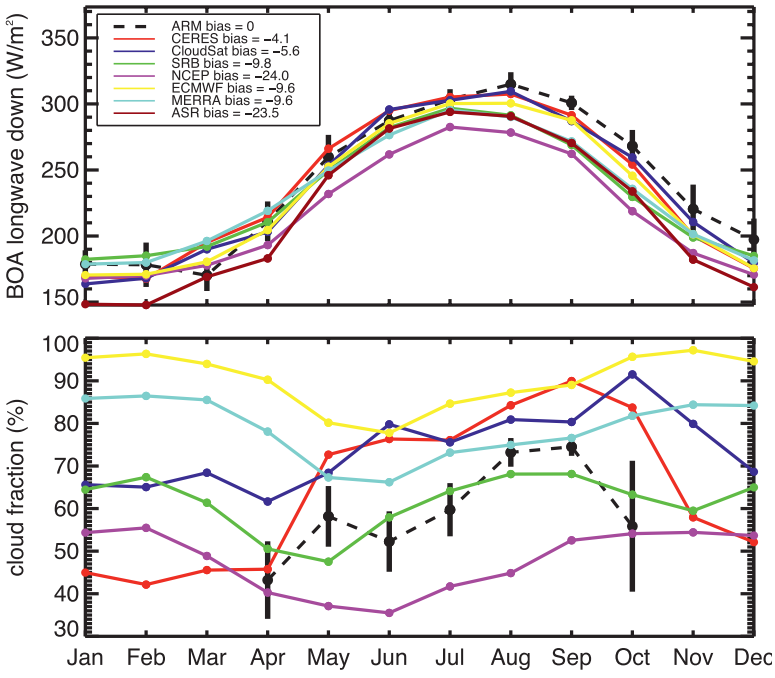

Fig. 2. Monthly mean (top) surface downwelling longwave radiation (BOA-LWDN), and (bottom) all-sky cloud fraction averaged over the period between 2007 and 2010. ARM measurements (dashed black line) are obtained from Barrow, Alaska, on the North Slope (71.3°N, 156.6°W). Cloud fraction was measured from the ARM site using the all-sky imager. CERES (red), *CloudSat* (blue), GEWEX-SRB (green), NCEP (pink), ECMWF (yellow), MERRA (teal), and ASR (maroon) products are matched to the nearest 2.5° region. Error bars were determined from the standard deviation taken from the population of ARM site observations.

EXAMPLE APPLICATIONS. Most of the A-Train satellite products now span over a decade of observations. When used in conjunction with the longer time series of reanalysis and/or previous satellite datasets (e.g., GEWEX-SRB used here), multiple decades of information can be used to study a variety of applications geared to evaluate climate change. We provide a few examples illustrating these applications below.

Validating surface radiative fluxes using ARM data. Validation studies are key to ensuring the successful implementation of retrieval techniques and parameterizations used in satellite and reanalysis data. The ArORIS dataset provides opportunities to validate satellite and reanalysis data from numerous ground-based instruments across multiple climate zones. In this example, we use the ARM site located on the North Slope of Alaska near Barrow (71.3°N; 156.6°W). Surface radiative flux and all-sky cloud fraction comparisons are made with satellite and reanalysis data using the nearest matched 2.5° region. The ARM site contains a suite of instruments that measure cloud properties and radiative fluxes at an hourly temporal resolution. These measurements were averaged to monthly values to match the satellite and reanalysis sampling period. Figure 2 shows the annual cycle of the mean downwelling thermal radiation measured by a pyrgeometer and overhead cloud fraction measured using a total sky imager. Here, we find a consistent negative bias in downwelling longwave radiation received at the surface in all products, especially in reanalysis products.

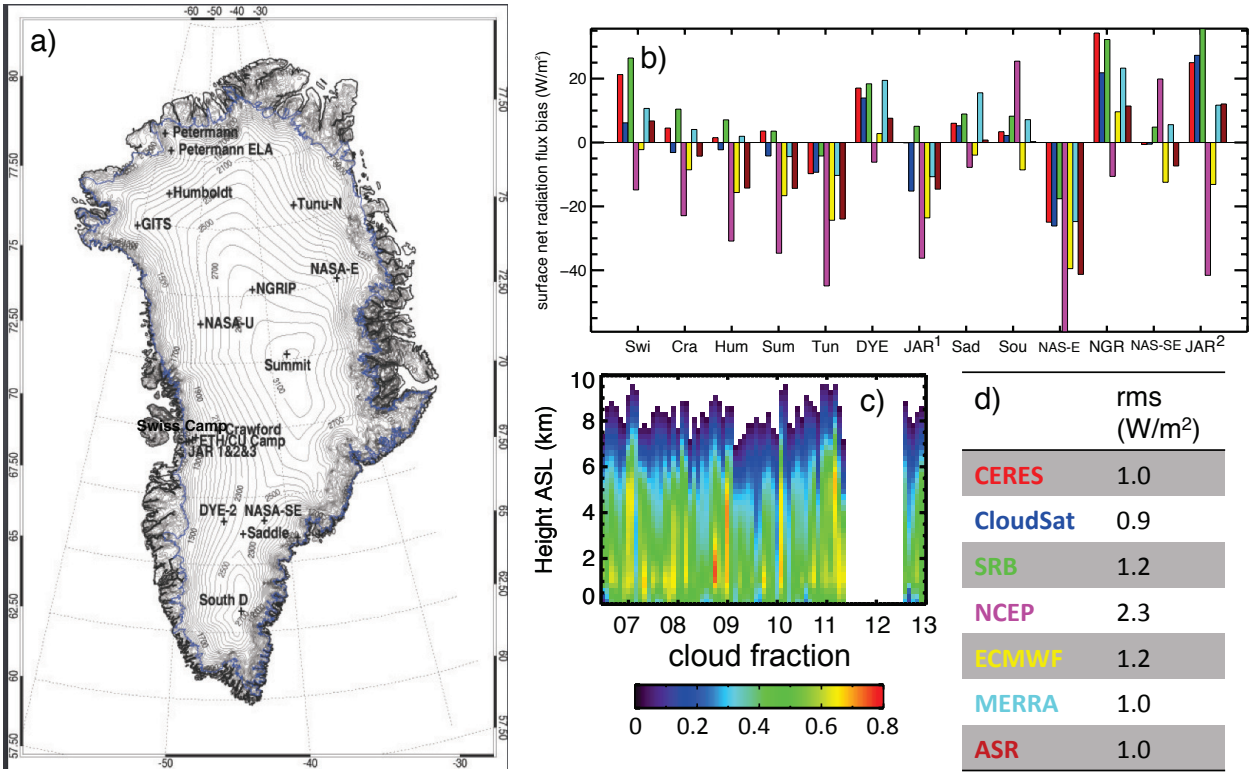

Fig. 3. (a) Location of the Greenland Climate Network (GCnet) ground-based instruments used to construct the surface net radiation annually average biases between GCnet and the collocated measurements from satellite and reanalysis products. (b) Biases are derived from the differences in the monthly means calculated from the 2007–10 period (CERES, red; *CloudSat,* blue; GEWEX-SRB, green; NCEP, pink; ECMWF, yellow; MERRA, teal; ASR, maroon). (c) Monthly cloud-cover fraction over Greenland derived from *CloudSat*/*CALIOP* is binned as a function of height above the surface. (d) The root-mean-square error in the net surface radiation for each product is calculated by averaging the bias from all ground-based sites. Panel (a) was obtained from the Cooperative Institute for Research in Environmental Sciences web page.

Negative biases like these are commonly observed in validation studies focusing on regions where extremely cold air drastically reduces the water vapor absorption continuum, which complicates the treatment of thermal emission in radiative transfer models. Despite the significantly larger cloud fraction (and variability) in many of the reanalysis products, the downwelling longwave radiation is still too small at the surface. For a detailed analysis, we recommend using the higher-resolution products within ArORIS to compare the point-source ARM measurements with the other data products. These results demonstrate that detailed observations of clouds and radiation from ARM sites can provide invaluable information to validate and improve cloud and radiation parameterization schemes used in satellite, and in particular, reanalysis products.

Validating surface radiative fluxes using the Greenland Climate Network. In general, climate models and reanalysis products are tuned to the top of atmosphere radiation budget as measured by satellite observations. By contrast, the surface budget cannot be tuned to the same extent due to unknown energy constraints from sparsely measured data. We employ the same approach as the previous example except now using a unique network of Greenland surface-based radiation sensors to provide a robust assessment of the bias with respect to the surface. Figure 3a shows the location of more than 20 stations throughout Greenland. These sites are then matched to the nearest grid cell and observations averaged over each month for comparison with other ArORIS products. This method underscores several prominent features. For example, the bias is smallest using the *CloudSat*/

CALIOP product because it can accurately sample the vertical distribution of cloud fraction and can estimate the associated cloud water content (Fig. 3c), both of which strongly modulate radiative fluxes. It therefore has great potential to estimate the surface radiation over the Arctic. For reanalysis products, MERRA has the highest accuracy with respect to the Greenland Climate Network while NCEP performs the worst (Fig. 3d). Due to its broad swath, CERES provides reliable data over the whole Arctic and serves as a key benchmark for assessments of the surface radiation budget in this region.

Science application—sea ice albedo feedback. Over the past century, the Arctic has undergone accelerated warming compared to the global mean rise in surface temperature. Part of this response is hypothesized to have arisen from a sea ice albedo feedback mechanism. As surface temperatures rise, sea ice melts and exposes more of the darker ocean, which can then absorb more solar radiation, causing greater heating and melting (Fig. 4), although evaporative cooling of the surface increases somewhat due to the increased open-ocean surface area. Over the past decade, cloud fraction has increased on average during summer months in all of the data products (Fig. 4b). But because clouds are brighter than the darker exposed ocean, they can act to "buffer" the strength of the sea ice albedo feedback as cloud fraction increases. However, despite the increase in cloud fraction, the absorbed solar radiation has continued to increase in all data products (Fig. 4c), and these changes virtually mimic the changes resulting from a substantial loss of sea ice extent. The ArORIS dataset can be used to analyze other seasons or in joint assessments with regional climate models to help unravel the nature of the sea ice albedo feedback in the Arctic.

Assessment—radiation budget. Earth's radiation budget is a concept used for understanding how much energy the Earth receives from the Sun and how much energy the Earth system radiates back to space as thermal radiation. When averaged over the globe, the incoming radiation must balance the outgoing radiation to maintain equilibrium. Having accurate measurements of the radiation budget is critical in order to monitor and measure any radiative flux imbalance caused by global warming. Because the Arctic receives less sunlight than lower latitudes, a net flux of energy is needed in order to maintain global radiative equilibrium. Figure 5 shows the various radiative fluxes for the Arctic for each of the integrated products in the ArORIS dataset. General features of this figure reveal the following: top-of-atmosphere radiative fluxes are well constrained; surface downwelling longwave radiation tends to be underestimated in reanalysis

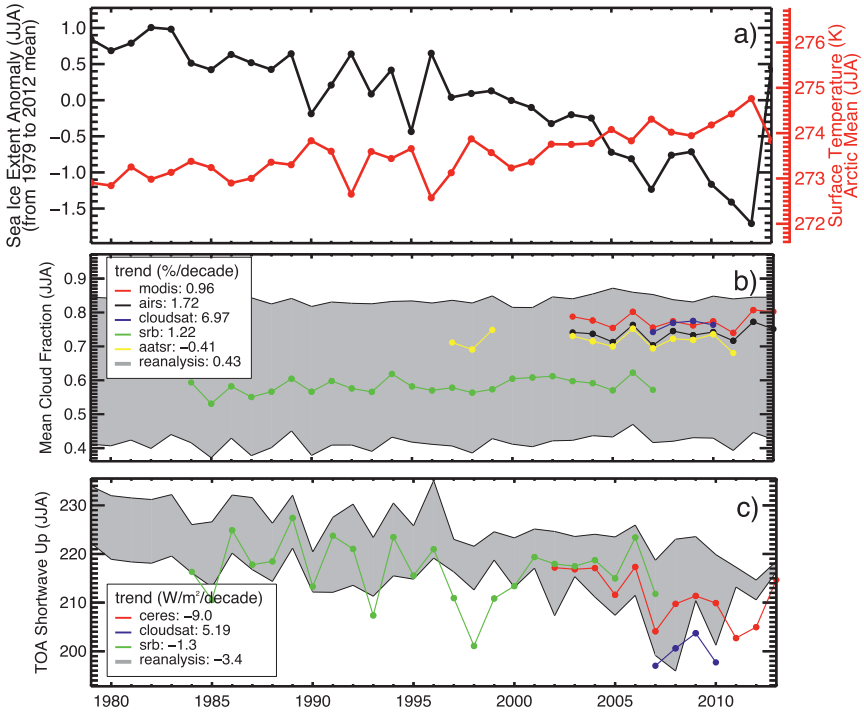

FIG. 4. Binned JJA (June, July, August) average (a) NSIDC sea ice extent anomaly, and (b) mean all-sky cloud cover fraction and (c) top-of-atmosphere reflected shortwave radiative flux calculated from 70°N to 90°N using satellite and reanalysis products [CERES, red; *CloudSat*, blue; AIRS, black; GEWEX-SRB, green; (A)ATSR; yellow; reanalysis, gray, which comprises the mean of NCEP, ECMWF, and MERRA]. Trend regression slope values are calculated using the entire length of the time series for each individual product. The temporal sampling period differs for each data product. *CloudSat* averages are based on 70°–82°N.

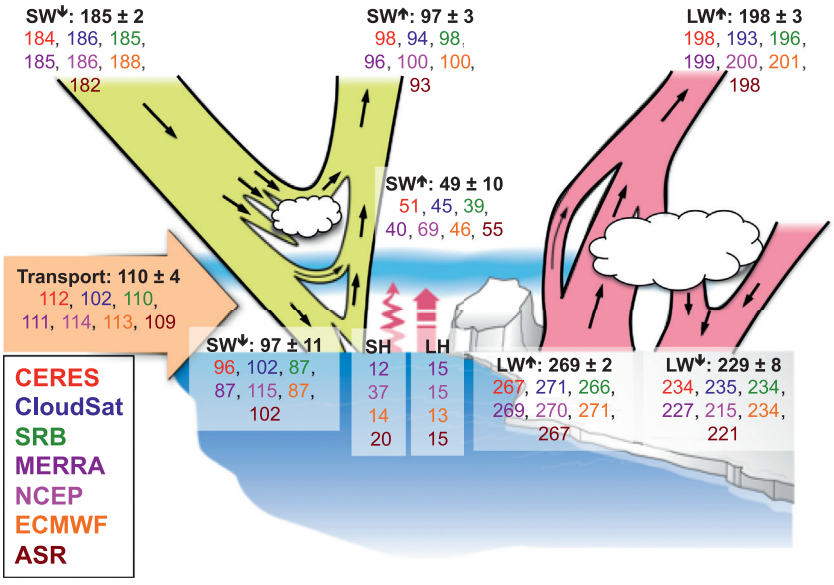

Fig. 5. Schematic diagram of the energy budget depicted for the Arctic (70°–82°N). Yellow, pink, and orange streams denote the shortwave (sw) and longwave (lw) top- and bottom-of-the-atmosphere (TOA and BOA) upwelling (upward direction black arrow) and downwelling (downward direction black arrow) radiative fluxes. Squiggly and broken upward arrows denote the sensible heat (SH) and latent heat (LH) fluxes, respectively. Large orange arrow denotes the poleward heat transport to the Arctic. Annually averaged estimates of the radiative fluxes were calculated for the period 2007–10 using satellite and reanalysis products (CERES, red; *CloudSat,* blue; GEWEX-SRB, green; NCEP, pink; ECMWF, yellow; MERRA, teal; ASR, maroon; black is the ensemble mean of all datasets) where available. Means and standard deviations were calculated from the ensemble of the products and listed in the diagram next to each radiative flux stream.

products compared to the satellite measurements; surface downwelling shortwave radiation is more variable (±6%) than the top-of-atmosphere budget, presumably due to large variations in cloud fraction; NCEP reanalysis tends to be a significant outlier in all flux calculations; and the ASR reanalysis product tends to perform the best, with the smallest overall RMS value with respect to CERES. Given the higher spatial and temporal resolution, the ASR product can capture complex terrain and diurnal variations more reliably than the other reanalysis products. This suggests that higher-resolution models may improve radiative flux estimates over the Arctic.

Assessment—moisture budget. The conjoining of radiation and moisture budgets completes the assessment of the Earth's energy budget. Moisture cycles through many different reservoirs on the Earth (e.g., snow/ice, fresh water, saline water, and atmospheric water) and is highly variable over seasonal and longer-term time scales compared to radiation fluxes. Heat is exchanged between the surface and the atmosphere through precipitation and latent and sensible heat fluxes. Figure 6 shows the dominant processes of the hydrological cycle over land and ocean regions in the Arctic. General features include the following: precipitation outweighs evaporation, thereby leading to net atmospheric transport of moisture from lower latitudes into the Arctic; precipitation and evaporation tend to be larger over the ocean compared to land; and more precipitation falls on the land than is lost via runoff and evaporation/sublimation, thereby leading to accumulation during the period of 2007–10. The range of uncertainty in oceanic precipitation rate among the products is estimated to be ±10% using one standard deviation divided by the mean value. Regions containing numerous rain gauges provided by the GPCC product may be useful for improving and constraining estimates over land. To improve overall assessments of the Earth's energy budget as the climate changes, it is imperative to close the gap of this fairly large uncertainty by maintaining and continually improving the current monitoring systems.

SUMMARY AND DATA ACQUISITION. The primary purpose of developing ArORIS is to bring together satellite, reanalysis, and in situ measurements into a common framework to encourage a comprehensive approach for pinning down uncertainties related to climate change. The dataset is geared for long-term assessment and validation of satellite and reanalysis products, and satellite comparisons with global circulation models, scientific inquiry, and assessments of the Earth's radiation and moisture budgets. A few examples demonstrating the potential usefulness of this new dataset were presented in this article. The dataset will be updated periodically in order to include

the most recent observations and advances in product development. The matched products listed in Table 1 are available for download and are approximately 7 GB in size. ArORIS is currently staged at the Cooperative Institute for Research in the Atmosphere (CIRA) CloudSat web page portal for data acquisition (www.cloudsat.cira.colostate.edu/community-products/arctic-observation-and-reanalysis-integrated-system) along with detailed product documentation.

ACKNOWLEDGMENTS. We thank the following distribution centers for the data used to construct this product: NASA Goddard Earth Sciences Data and Information Center for AIRS, MODIS, MERRA, and GLDAS products; Centre for Environmental Data Analysis (CEDA) for ATSR-2 and AATSR ESA CCI_Cloud (European Space Agency Climate Change Initiative Cloud) products; CIRA for *CloudSat* data products; NASA Langley Research Center for CERES, GEWEX-SRB, and CALIOP data products; Jet Propulsion Laboratory (JPL) for GRACE products; National Snow and Ice Data Center, NOAA Earth System Research Laboratory for CMAP, GPCP, NCEP, GPCC, and climate indices; Automated Mutual-Assistance Vessel Rescue center for shipping data; National Center for Atmospheric Research for ASR; European Centre for Medium-range Weather Forecasts for ECWMF and MACC products; Climate Research Facility for ARM data; and the Cooperative Institute for Research in Environmental Sciences for GCNET products. We would also like to thank our programmer, Ryan Fuller, for his input and contributions to the construction of this integrated dataset. Part of the research was carried out at Colorado State University under NASA Grant NAS5-99237, and the other portion at JPL, Caltech, under a contract with NASA funded by Grant NNN13D771T and JPL CloudSat Subcontract 1439268.

FOR FURTHER READING

Brutel-Vuilmet, C., M. Ménégoz, and G. Krinner, 2013: An analysis of present and future seasonal Northern Hemisphere land snow cover simulated by CMIP5 coupled climate models. *The Cryosphere,* **7,** 67–80, doi:10.5194/tc-7-67-2013.

Henderson, D. S., T. L'Ecuyer, G. Stephens, P. Partain, and M. Sekiguchi, 2013: A multisensor perspective on the radiative impacts of clouds and aerosols. *J. Appl. Meteor. Climatol.*, **52,** 853–871, doi:10.1175/JAMC-D-12-025.1.

Kay, J. E., and T. L'Ecuyer, 2013: Observational constraints on Arctic Ocean clouds and radiative fluxes during the early 21st century. *J. Geophys. Res.*, **118,** 7219–7236, doi:10.1002/2013JA019042.

Serreze, M. C., and R. G. Barry, 2009: *The Arctic Climate System,* Cambridge University Press, 404 pp.

Stephens, G. L., and Coauthors, 2012: The global character of the flux of downward longwave radiation. *Nat. Geosci.,* **5,** 691, doi:10.1038/ngeo1580.

Stroeve, J. C., V. Kattsov, A. P. Barrett, M. C. Serreze, T. Pavlova, M. M. Holland, and W. N. Meier, 2012: Trends in Arctic sea ice extent from CMIP5, CMIP3 and observations. *Geophys. Res. Lett.,* **39,** L16502, doi:10.1029/2012GL052676.

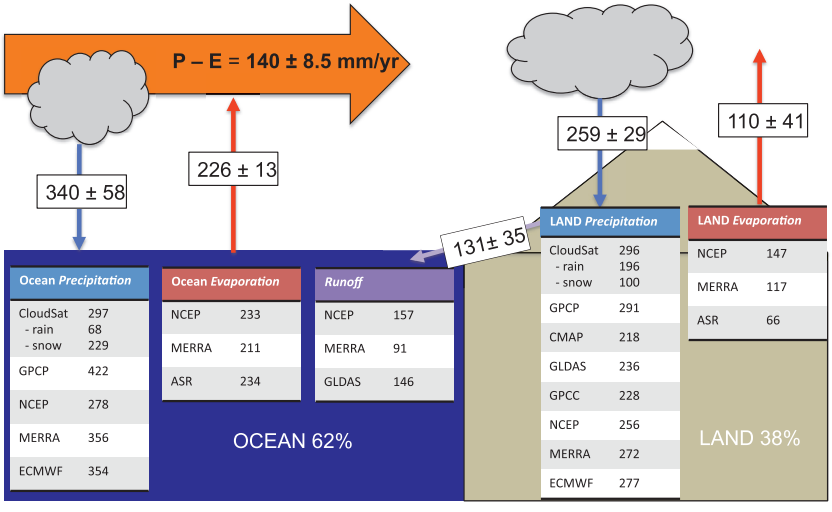

Fig. 6. Schematic diagram of the hydrological cycle depicted for the Arctic (70°–82°N). Precipitation (downward blue arrow) and evaporation (upward red arrow) were estimated over land and ocean regions separately. Calculations were weighted by both the cosine of the latitude and fraction of land in each grid. Runoff (purple arrow) is estimated over land, and precipitation minus evaporation was estimated over the entire Arctic region. Annually averaged estimates of the moisture fluxes were calculated for the period 2007–10 using *CloudSat,* GPCP, GPCC, GLDAS, CMAP, NCEP, MERRA, ECMWF, and ASR (where available).